Progressive fault identification and prognosis of railway tracks based on intelligent inference
Research Area: #1 Transportation

Final Report
July 2022

Principal Investigator: Jiong Tang

Department of Mechanical Engineering
University of Connecticut

Author: Jiong Tang, Yang Zhang, Ting Wang

Sponsored By
Transportation Infrastructure Durability Center
List other Sponsors if applicable (i.e. MaineDOT)

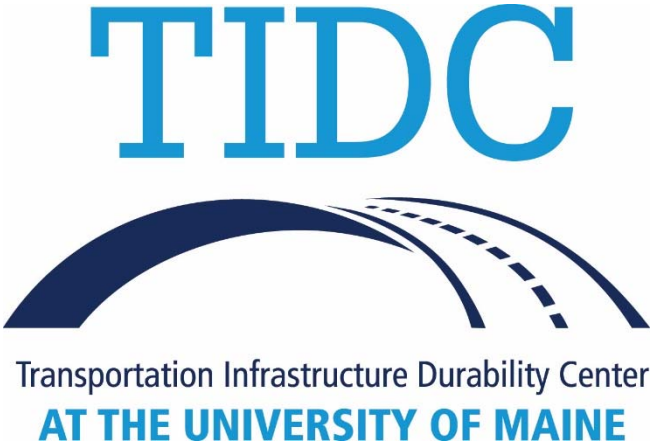

A report from
University of Connecticut
Department of Mechanical Engineering
191 Auditorium Road
Storrs, CT 06269
Phone: (860) 486 5911
Website: https://dscl.uconn.edu

About the Transportation Infrastructure Durability Center

The Transportation Infrastructure Durability Center (TIDC) is the 2018 US DOT Region 1 (New England) University Transportation Center (UTC) located at the University of Maine Advanced Structures and Composites Center. TIDC's research focuses on efforts to improve the durability and extend the life of transportation infrastructure in New England and beyond through an integrated collaboration of universities, state DOTs, and industry. The TIDC is comprised of six New England universities, the University of Maine (lead), the University of Connecticut, the University of Massachusetts Lowell, the University of Rhode Island, the University of Vermont, and Western New England University.

U.S. Department of Transportation (US DOT) Disclaimer

Acknowledgements

Funding for this research is provided by the Transportation Infrastructure Durability Center at the University of Maine under grant 69A3551847101 from the U.S. Department of Transportation's University Transportation Centers Program. [Include any acknowledgements for other contributors (i.e. your university or contributing DOTs/industry partners) here.]

Technical Report Documentation Page

1. Report No.	**2. Government Accession No.**	**3. Recipient Catalog No.**
4 Title and Subtitle Progressive fault identification and prognosis of railway tracks based on intelligent inference		**5 Report Date** **6 Performing Organization Code**
7. Author(s) Jiong Tang https://orcid.org/0000-0002-6825-9049 Yang Zhang and Ting Wang		**8 Performing Organization Report No.**
9 Performing Organization Name and Address University of Connecticut, Storrs, CT 06269		**10 Work Unit No. (TRAIS)** **11 Contract or Grant No.**
12 Sponsoring Agency Name and Address		**13 Type of Report and Period Covered** **14 Sponsoring Agency Code**

15 Supplementary Notes

16 Abstract In this project we explore and develop a new damage detection and identification approach suitable for elastic structure which is built upon piezoelectric active interrogation and intelligent data analytics. Novel sensor designs have been accomplished to effectively extract the impedance information of the underlying structure, the change of which provides the input information for the subsequent damage identification analysis. A series of highly accurate and robust damage identification algorithms built upon multi-objective optimization and Bayesian inference is then formulated to identify the location and severity of damage. During the investigation, new energy harvesting scheme that can enhance the electro-mechanical coupling of the transducer is synthesized, which can lead to enlarged actuation/sensing range. Comprehensive experimental investigations are conducted to validate the sensor prototype design as well as the algorithmic advancements. Throughout the research, industrial insights are adopted to improve the system performance. This research leads to a new structural fault identification methodology that has potential to be applied to large scale infrastructure, including but not limited no railway tracks.

17 Key Words Structural damage identification, piezoelectric transducer, sensor, impedance measurement, inverse analysis, multi-objective optimization, energy harvesting, electro-mechanical coupling, damage location, damage severity

18 Distribution Statement
No restrictions. This document is available to the public through

19 Security Classification (of this report)	**20 Security Classification (of this page)**	**21 No. of pages**	**22 Price**
Unclassified	Unclassified	24	

Form DOT F 1700.7 (8-72)

Contents

List of Figures

List of Tables

List of Key Terms

Structural damage identification, piezoelectric transducer, sensor, impedance measurement, inverse analysis, multi-objective optimization, energy harvesting, electro-mechanical coupling, damage location, damage severity

Abstract

In this project we explore and develop a new damage detection and identification approach suitable for elastic structure which is built upon piezoelectric active interrogation and intelligent data analytics. Taking advantage of their two-way electro-mechanical coupling, we integrate piezoelectric transducers to the host structure to conduct simultaneous actuation and sensing. As piezoelectric transducers feature high bandwidth, they are capable of actuating and sensing the structure in high-frequency (kHz) range, leading to high sensitivity toward small-sized damage. Novel sensor designs have been accomplished to effectively extract the impedance information of the underlying structure, the change of which provides the input information for the subsequent damage identification analysis. A series of highly accurate and robust damage identification algorithms built upon multi-objective optimization and Bayesian inference is then formulated to identify the location and severity of damage. During the investigation, new energy harvesting scheme that can enhance the electro-mechanical coupling of the transducer is synthesized, which can lead to enlarged actuation/sensing range. Comprehensive experimental investigations are conducted to validate the sensor prototype design as well as the algorithmic advancements. Throughout the research, industrial insights are adopted to improve the system performance.
This research leads to a new structural fault identification methodology that has potential to be applied to large scale infrastructure, including but not limited no railway tracks.

Chapter 1: Introduction and Background

1.1 Project Motivation

Infrastructure components are often of large scale, such as railway tracks and bridge components. The safe operation of these components hinges upon their structural integrity. A variety of material/structural defects, typically with very small size and signature, could occur. Traditionally, to detect and identify these defects, labor intensive inspections and maintenances were required. Moreover, as defects usually progress over time, constant inspections are necessary. As such, traditional labor intensive inspection and maintenance schemes are extremely costly, yet ineffective and inefficient in dealing with the new situations/threats to safeguard the infrastructure. There is urgent need to develop novel sensing mechanisms and new sensors to facilitate autonomous and robust fault identification and prognosis. In recent years, the advent of smart transducers such as piezoelectric transducers has led to transformative advancement in the realm of structural health monitoring. Indeed, piezoelectric transducers feature two-way electro-mechanical coupling. They can be used as actuators when subject to voltage excitation, and can also be used as sensors when deformed. This gives rises to the idea of active interrogation. That is, we embed a piezoelectric transducer with the host structure and apply voltage excitation to induce structural vibration. If the host structure has damage, the vibratory response which is sensed by the same piezoelectric transducer will exhibit change. The change of structural responses can be used as input for inverse analysis to identify the location and severity of structural damage. The piezoelectric transducers can function in high-frequency range with small characteristic wavelength. Thus they are capable of reflecting the effect of small-sized damage. Meanwhile, the recent progress in computing power has triggered a variety of intelligent data analytics methods which can be potentially extended to structural damage identification based on the aforementioned active interrogation. Obviously, the combination of new transducer development and the dramatically improved computational capability is highly promising for infrastructure diagnosis and prognosis. Fundamentally, this may lead to autonomous and highly accurate structural damage identification which can solve the current challenge of labor intensive inspection and maintenance.

1.2 Research, Objectives, and Tasks

The overarching goal of this project is to develop a completely new, autonomous damage identification sensory system that can accurately and robustly identify structural damage in large-scale infrastructure components. We aim at taking advantage of the latest progresses in smart transducers and computing power, and leverage upon mechatronic synthesis and computational intelligence. Our specific objectives are

a. Explore new active sensing mechanisms and formulate analysis and design methodologies;
b. Develop new physics-informed inference algorithms to realize highly accurate fault diagnosis and prognosis.

To accomplish these objectives, research activities along two thrust areas are executed, sensor design and synthesis with energy harvesting capacity, and damage identification algorithmic investigation. Four tasks are conducted:

Task 1: Sensing mechanism development
Task 2: Sensor-node energy harvesting
Task 3: Sensor networking strategy
Task 4: Highly accurate and robust decision making

1.3 Report Overview

In the subsequent chapters, we present the research methodology and results obtained throughout this research.

Chapter 2 outlines the materials involved in this research. The sensor design and analyses are based upon correlated finite element modeling and experimental investigation. Damage identification is conducted through multi-objective optimization approach. The experimental testbeds are summarized.

Chapter 3 presents in detail the research tasks as well as the key data/results. The finite element modeling of sensor-structure interaction is developed. At sensor node level, piezoelectric energy harvesting is established, followed by design improvement featuring enhanced electromechanical coupling through the synthesis of self-powering negative capacitance. Sensor networking and structural damage identification are then presented with details of the latest advancement of multi-objective optimization based inverse analysis. All the results are validated experimentally.

Chapter 4 summarizes the workforce training aspect of the project as well as knowledge dissemination.

Chapter 5 provides the overall conclusion as well as recommendation for future work

Chapter 2: Methodology

2.1 Materials

In terms of physical materials, this project involves piezoelectric transducers used as actuators and sensors concurrently, circuitry elements including op-amps that are connected with the piezoelectric transducers to facilitate actuation and sensing to enable active interrogation, host structures made of aluminum beams and plates, as well as power supply data acquisition equipment.

In terms of reporting materials, in this final report we provide details of

a) sensor design configuration;
b) finite element analysis procedure of sensor-structure interaction;
c) circuitry design for self-powering energy harvesting and analysis; and
d) structural damage identification algorithms based on multi-objective optimization methodology and case studies.

2.2 Test Setup & Process

A number of testings are conducted throughout this project. Figure 1 shows the sensor design, in which a piezoelectric transducer is attached to a host structure to facilitate active interrogation. A small resistor is connected in serial with the transducer to acquire the current measurement which will then yield impedance/admittance measurement for structural damage identification. Correlated experimental investigations and finite element analyses are performed to elucidate the sensing mechanism and performance.

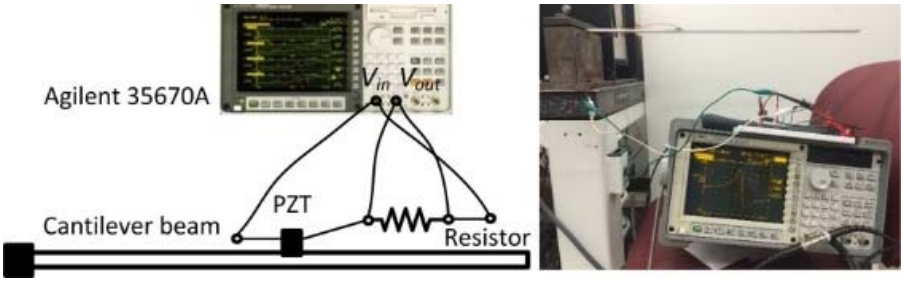

Figure 1 Host structure integrated with piezoelectric transducer and measurement circuitry with small resistor. The piezoelectric transducer is actuated with power supply and the circuitry dynamics is measured. As the transducer is electromechanically coupled with the host structure, the structural defect is reflected in the impedance/admittance information measured.

Figure 2 illustrates the combination of energy harvesting and negative capacitance to enable high electromechanical coupling with self-powering capacity. In this testing, the focus is on the development of piezoelectric energy harvesting that can lead to sensor autonomy with higher signal-to-noise ratio. The setup includes scanning laser vibrometer and auxiliary measurement devices to allow the in-depth analysis of circuitry dynamics.

Figure 3 showcases the structural damage identification testing. Aluminum beams and plates are employed as the host structures to develop and examine the damage identification algorithms developed. It is concluded that the proposed sensing mechanism and the new multi-objective

optimization based algorithms can identify the location and severity of faulty conditions accurately and robustly.

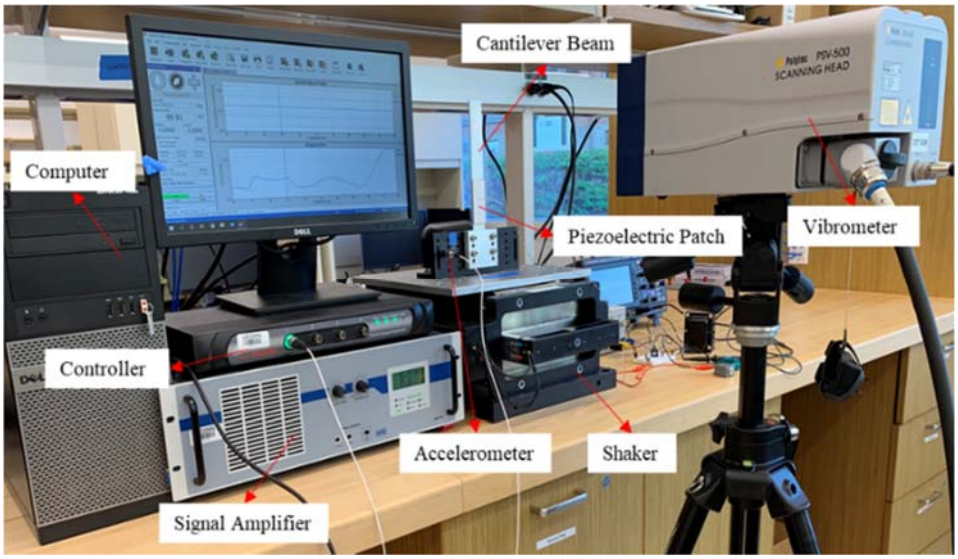

Figure 2 Experimental investigation of enhancing piezoelectric electromechanical coupling with self-powered negative capacitance. The negative capacitance can effectively increase the electromechanical coupling thereby enhancing the signal-to-noise ratio of active interrogation. A negative capacitance element requires power supply. We demonstrate that the piezoelectric transducer's energy harvesting capacity can ensure the self-sustainability of negative capacitance element, leading to an autonomous design.

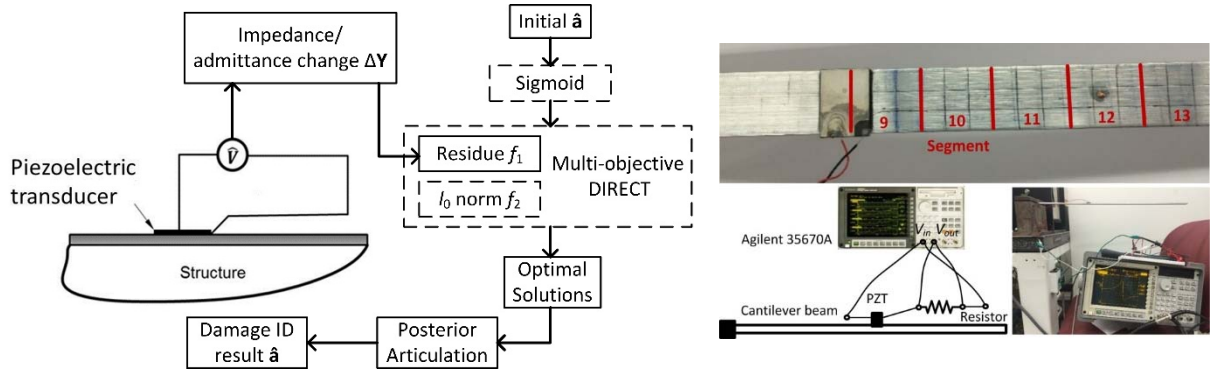

Figure 3 Illustration of structural damage identification using piezoelectric active interrogation. The sensor node collects the impedance/admittance information that carries the damage signature. A series of multi-objective optimization algorithms are developed to identify the location and severity of damage occurrence.

The details of the analyses and testings are reported in Chapter 3.

Chapter 3: Results and Discussion

3.1 Sensor design, analysis, and energy harvesting for enhanced electromechanical coupling

While both piezoelectric impedance and admittance can be used as information carrier for damage identification, here we use the piezoelectric admittance, i.e., the reciprocal of the electric impedance, as the response of interest. Consider Figure 1. The equations of motion of the host structure integrated with piezoelectric transducer can be derived as [1]

$$\mathbf{M}\ddot{\mathbf{q}} + \mathbf{C}\dot{\mathbf{q}} + \mathbf{K}\mathbf{q} + \mathbf{K}_{12}Q = \mathbf{0} \tag{1a}$$

$$R\dot{Q} + K_c Q + \mathbf{K}_{12}^T \mathbf{q} = V_{in} \tag{1b}$$

where $\mathbf{q}$ is the displacement vector, k_c is the inverse of the capacitance of the piezoelectric transducer; $\mathbf{K}_{12}$ is the electromechanical coupling vector, $\mathbf{K}$, $\mathbf{C}$, $\mathbf{M}$ are the stiffness, damping and mass matrices, respectively, and Q is the electrical change on the surface of piezoelectric patch. In this research, we define damage as percentage change of stiffness in the segment. The stiffness matrix with damage occurrence in structure, $\mathbf{K}_d$, can be then expressed as $\mathbf{K}_d = \sum_{i=1}^{n} \mathbf{K}_h^i \left(1-\alpha_i\right)$. $\mathbf{K}_h^i$ is the stiffness matrix of ith segment under the healthy state. $\alpha_i \in [0,1]$ is the damage index indicating the stiffness loss of the ith segment, which is the unknow to be identified. n is the total number of segments. Thus, the piezoelectric admittance when damage occurs can be written as

$$y_d^c(\omega) = \frac{\dot{Q}}{V_{in}} = \frac{j\omega}{j\omega R + k_c + \mathbf{K}_{12}^T\left(\mathbf{K}_d + j\omega\mathbf{C} - \omega^2\mathbf{M}\right)\mathbf{K}_{12}} \tag{2}$$

where j refers to the imaginary unit. Under the assumption of linear relationship between admittance variation, we can use Taylor series expansion to expand the admittance in terms of the damage index, in which the higher terms are ignored here since small damage is assumed. The vector of admittance change can be obtained at the set of excitation frequencies, $\boldsymbol{\omega} = \{\omega_1, \ \omega_2, \ \ldots, \ \omega_m\}$, in matrix form as [2,3]

$$\Delta y^c{}_{m\times 1} = \begin{bmatrix} \Delta Y(\omega_1) \\ \vdots \\ \Delta Y(\omega_m) \end{bmatrix} = \mathbf{S}_{m\times n}\boldsymbol{\alpha}_{n\times 1} \tag{3}$$

where $\mathbf{S}$ is the sensitivity matrix. Similarly, we denote $y^p(\boldsymbol{\omega}) = \left[y^p(\omega_1), \ \ldots, \ y^p(\omega_m)\right]^T$ as the piezoelectric admittance measurements.

Throughout this research, comprehensive numerical analyses are conducted based upon finite element discretization. The numerical results are then correlated to experimental results through model updating which is built upon matching the dynamic characteristics including resonant frequencies, damping ratio and resistance, as well as boundary conditions. Shown in Figure 4 is one representative case, in which the admittance responses around certain structural resonances are simulated successfully and match perfectly with experimental results upon model updating.

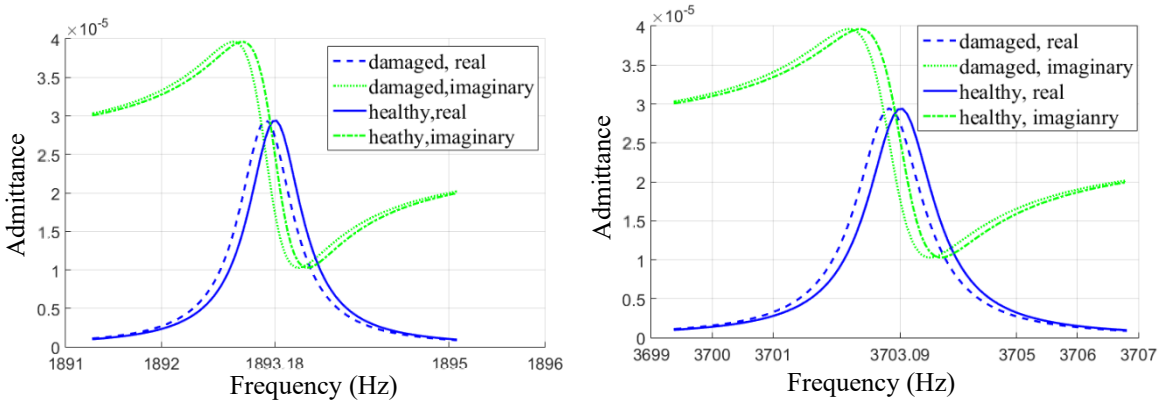

Figure 4 Finite element based piezoelectric admittance response simulation before and after damage occurrence. Structural damage causes noticeable change of the admittance responses.

The physics-based finite element analysis provides guidance for transducer sizing and location analysis, and lays down a foundation of the subsequent inverse analysis reported in the next subsection.

A very important aspect of this project is the sensor autonomy which requires high signal-to-noise ratio and minimized power supply. One reason we choose to utilize piezoelectric transducer for active interrogation is that it can be concurrently used to harvest ambient vibratory energy, i.e., converting mechanical vibration into electrical charge to be collected in a rechargeable battery. Therefore, at the sensor node level, we explore the integration of negative capacitance to enhance electromechanical coupling with self-powering energy harvesting.

Here we consider a unimorph piezoelectric transducer with RL shunt. As shown in Figure 5, the host structure is a cantilever beam. The piezoelectric transducer is equivalent to a voltage source in series with an inherent capacitance. When an inductor and a resistor are added into the piezoelectric shunt, a LC piezoelectric resonant shunt is formed. The circuitry diagram is illustrated in Figure 5 as well, combing the LC resonant circuit with the negative capacitance which is realized through the usage of op-amp [4,5].

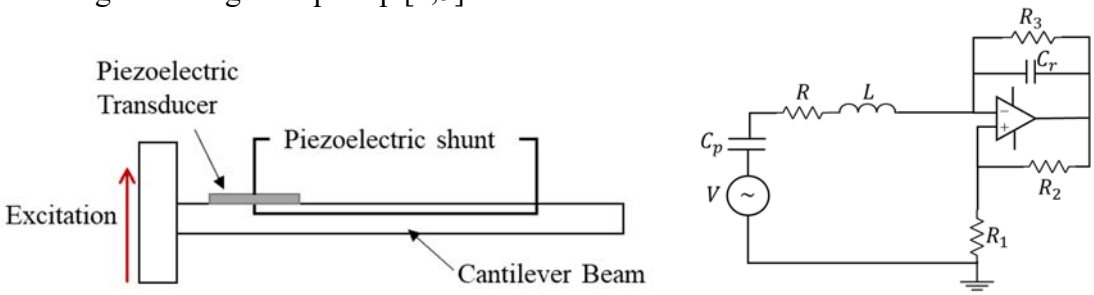

Figure 5 Piezoelectric circuit with negative capacitance.

Based upon the simplified model, the system equations can be written as [6]

$$\begin{cases} m\ddot{q} + c\dot{q} + kq + k_1 Q = F_m \\ L\ddot{Q} + R\dot{Q} + \hat{k}_2 Q + k_1 q = 0 \end{cases} \tag{4}$$

where q and Q are displacement and charge variables. m, k, and c are system equivalent mass, stiffness, and damping coefficients. k_1 represents the electro-mechanical coupling coefficient. F_m

is the external excitation force. L and R are the inductance and resistance values. $\hat{k}_2$ coefficient is related to both the inherent capacitance of the piezoelectric transducer C_p and the introduced negative capacitance value C_n, i.e., $\hat{k}_2 = 1/C_p - 1/C_n$.

In this research, without loss of generality the resistance and inductance are selected to be the optimal values for the optimal vibration suppression performance to ensure the reliable operation of the sensor, which are [7]

$$L_{\text{opt}} = \frac{m\hat{k}_2}{k}, R_{\text{opt}} = \frac{k_1\sqrt{2m\hat{k}_2}}{k} \tag{5}$$

Under harmonic excitation, the transfer functions of displacement and charge in frequency-domain can be obtained as

$$\begin{cases} \dfrac{\bar{q}}{\bar{F}_m} = \dfrac{-\omega^2 L + i\omega R + \hat{k}_2}{(-\omega^2 L + i\omega R + \hat{k}_2)(-\omega^2 m + i\omega c + k) - k_1^2} \\ \dfrac{\bar{Q}}{\bar{F}_m} = \dfrac{-i\omega k_1}{(-\omega^2 L + i\omega R + \hat{k}_2)(-\omega^2 m + i\omega c + k) - k_1^2} \end{cases} \tag{6a, b}$$

Hereafter the overbar indicates the magnitude of the corresponding variable.

The negative capacitance circuit employs an op-amp which requires power. In this research we propose to use the same piezoelectric transducer for energy harvesting purpose. While the specific energy harvesting realization can adopt a variety of existing schemes, here we focus on the feasibility of self-sustainable negative capacitance, and investigate the power available in the shunt circuit. Such power can be utilized to charge a rechargeable battery in the system. When the power harvested is greater than the power consumed by the op-amp employed in the negative capacitance circuit, the negative capacitance becomes self-sustainable. In energy harvesting research, commonly a resistor load is employed to quantify the energy harvesting capability. In order to ensure the optimal vibration control performance, the resistor load in this research is set as the optimal resistance shown in Equation (5). The transfer function of the available power from the resistor element in the shunt versus the base excitation can be expressed as [8]

$$\frac{\bar{P}_s}{\bar{F}_m^2} = \frac{\omega^2 k_1^3 \sqrt{2m\hat{k}_2}}{k\left[(-\omega^2 L + i\omega R + \hat{k}_2)(-\omega^2 m + i\omega c + k) - k_1^2\right]^2} \tag{7}$$

According to Figure 5, the negative capacitance value can be expressed as

$$-C_n = -rC_r = -\frac{R_2}{R_1} C_r \tag{8}$$

where C_r is the reference capacitance value, and C_n is the negative capacitance value. R_1 and R_2 are two resistances to determine the magnification r. To separate variable r from variable C_n for simplicity, here we set $R_2 = R_1$. Thus $r = 1$ and $C_n = C_r$. Usually, a relatively large resistance is selected for R_3, e.g., $R_3 = 10M\Omega$ in this research. The power consumption of the op-amp can be obtained based upon the output voltage and output current of the op-amp as

$$\frac{\bar{P}_{\text{op-amp}}}{\bar{F}_m^2} = \frac{\bar{V}_{\text{out}}}{\bar{F}_m} \cdot \frac{\bar{I}_{\text{out}}}{\bar{F}_m} \tag{9}$$

The op-amp is assumed to be ideal, i.e., there is no current going through the two input terminals of the op-amp and there is no voltage difference between two input terminals of the op-amp. Based upon the voltage divider rule and $R_2 = R_1$, the output voltage of op-amp is twice the input voltage of op-amp. Similarly, based upon the current division, the output current of the op-amp is the sum of the current going through the upper and the lower branch. At the inverting input terminal, with the ideal assumption of no current going into the op-amp, the current in the main shunt is the

negative value of output current of the upper branch. Combining the equations of output voltage and current with that of charge generated in the main shunt, we can derive the power consumption of op-amp as

$$\frac{\bar{P}_{\text{op-amp}}}{\bar{F}_m^2} = \frac{2k_1^2(1+i\omega R_1 C_n)}{(R_1 C_n)^2\left[(-\omega^2 L+i\omega R+\hat{k}_2)(-\omega^2 m+i\omega c+k)-k_1^2\right]^2} \tag{10}$$

The net power for self-sustainability can be obtained by calculating the magnitude difference between the available power in Equation (7) and the power consumption of op-amp in Equation (9). The final magnitude of the net power transfer function can be expressed as

$$\left|\frac{\bar{P}_{\text{net}}}{\bar{F}_m^2}\right| = \left|\frac{\bar{P}_s}{\bar{F}_m^2}\right| - \left|\frac{\bar{P}_{\text{op-amp}}}{\bar{F}_m^2}\right| \tag{11}$$

A self-sustainable negative capacitance can be achieved by ensuring positive net power, i.e., Equation (11) should be positive. Then the optional negative capacitance range can be obtained from solving the following inequality:

$$C_n^4 - C_p C_n^3 - \frac{2kC_p}{k_1^2} C_n^2 - \frac{2mC_p}{k_1^2 R_1^2} > 0 \tag{12}$$

We can find the critical negative capacitance value from the above equation by setting the net power to be zero. Therefore, the self-sustainable vibration suppression enhancement system with negative capacitance integration requires the negative capacitance value to be larger than the critical negative capacitance value.

Comprehensive investigations on circuitry dynamics and sensor-structure interaction are conducted to examine the self-powering negative capacitance and to elucidate the parametric influence. The experimental setup is shown in Figure 2. The cantilever beam (6061 Al) bonded with a piezoelectric patch (APC 850) is mounted on a shaker (APS 400). A controller (VR9500) is utilized to drive the power amplifier (APS 145) for shaker operation. An accelerometer (PCB 352C04) is glued on the shaker to make sure constant excitation acceleration. The circuitry responses are measured using an oscilloscope (Keysight DSOX1204G). The vibration responses are measured using a scanning laser vibrometer (Polytec PSV-500).

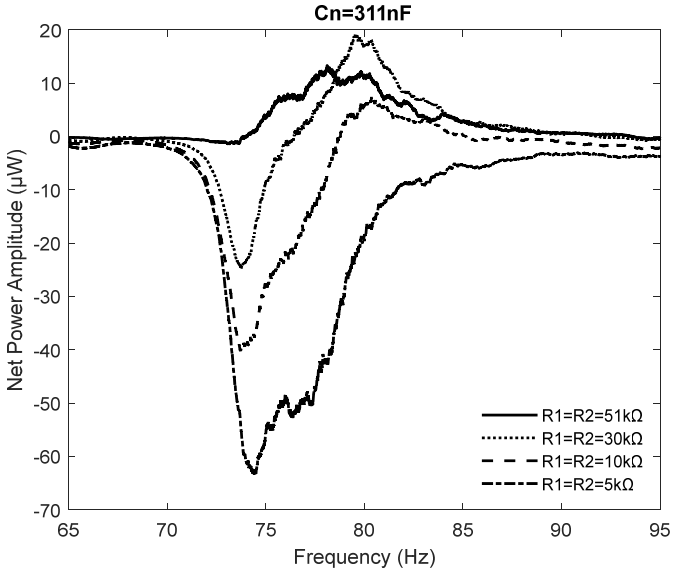

Figure 6 Net power increase by using larger resistance in negative capacitance circuit.

The beneficial effect of increasing resistance R_1 of the NC circuit on net power generation can be observed in Figure 6. With the same 311 nF NC value, when the resistance R_1 is increased, the frequency responses of the net power indeed change from completely negative, to partially positive, and then to entirely positive within the frequency range of interest. This matches very well to the analytical relationship between net power and resistance R_1. With the same negative capacitance value, self-sustainability can be enhanced by increasing the resistance R_1 of the negative capacitance circuit.

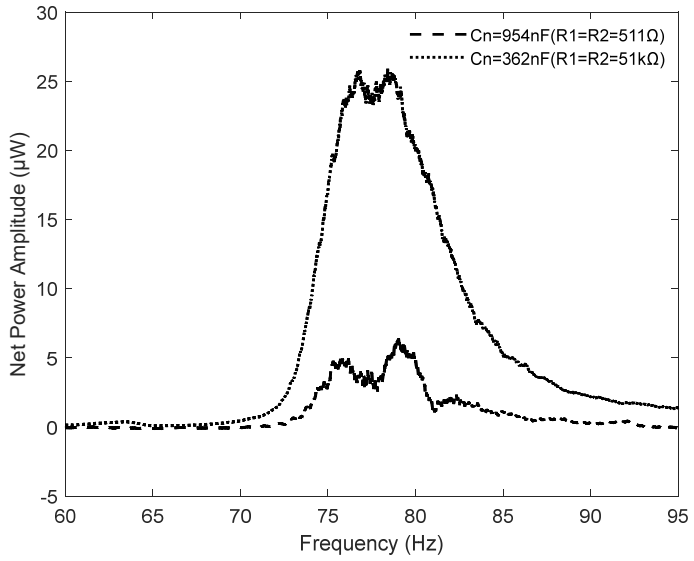

Figure 7 Net power performance under different negative capacitance values and R_1 values.

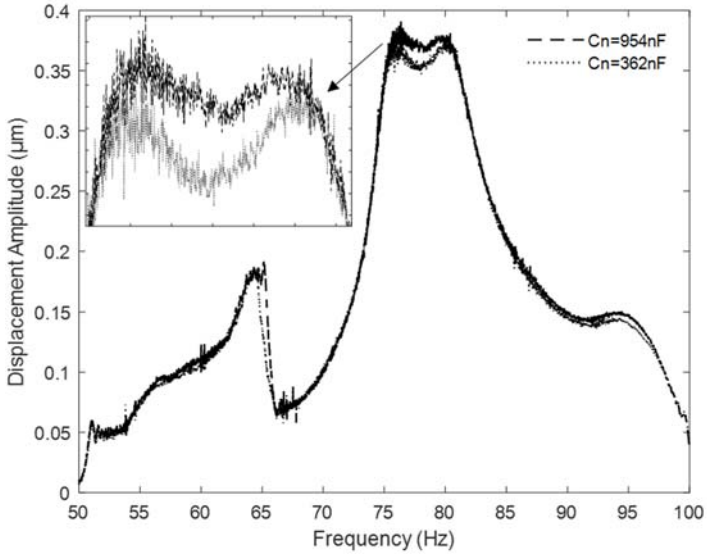

Figure 8 Vibration reduction performance owing to increased electro-mechanical coupling under different negative capacitance values and R_1 values.

To examine the simultaneous enhancements of both electromechanical coupling and self-sustainability, a large negative capacitance value (954 nF) with a small NC resistance $R_1 = 511\ \Omega$ is selected which corresponds to approximately point A in Fig. 5. Another much smaller negative

capacitance value (362 nF) with very large resistance $R_1 = 51\text{k}\Omega$ is selected to reflect the simultaneous enhancement happened at point D. The net power results under these two conditions are shown in Figure 7. Compared to the large negative capacitance value case (954 nF), the smaller negative capacitance value (362 nF) achieves a significant increase in net power magnitude, near five times, due to the application of large resistance $R_1 = 51\text{k}\Omega$.

The performance of electromechanical coupling enhancement and vibration reduction comparison between the aforementioned two negative capacitance values, 954 nF and 362 nF, are shown in Figure 8. When the negative capacitance value decreases from 954 nF to 362 nF, further vibration suppression can be observed around the resonant frequency, which is about 4.08%. The amount of enhancement depends on the negative capacitance value. When a very large resistance $R_1 = 51\text{k}\Omega$ is employed in the negative capacitance circuit, the critical negative capacitance value decreases to as small as 175.76 nF. The negative capacitance value can be selected even smaller than 362 nF for greater vibration suppression enhancement, as long as the negative capacitance value is greater than 175.76 nF.

The experimental results shown in in Figures 7 and 8 confirm that simultaneous enhancements of both vibration suppression and net power can be achieved by employing large resistance R_1 in the negative capacitance circuit. The negative capacitance can be selected freely within the proposed selection range. This is completely new finding, and benefit the sensor node design through enhanced electromechanical coupling with increased signal-to-noise ratio and further reduced vibration. These will enable the future development of completely wireless sensor nodes with autonomy.

3.2 Inverse analysis for structural damage identification

The effectiveness and robustness of sensing research hinges upon the inverse analysis algorithms which utilize the measurement information as input to generate the location and severity information as the output. Throughout this research, a series of inverse identification algorithms have been created. In this report, we summarize the latest advancement of a multi-objective optimization based algorithm to exemplify the progress.

Damage in a structure usually causes the change of admittance curve only around the resonant frequencies. As such, limited information can be used for damage identification. This makes structural damage identification an underdetermined problem. To solve this problem more effectively, we convert it into an optimization problem. By minimizing the difference between the experimental response of the structure and the predicted data from the numerical model in the parametric space, we can inversely identify the location and severity of the damage. Moreover, as damage occurs only in a small region of the structure, the damage indicator vector is generally sparse. Therefore, we build another objective function to minimize the number of damaged locations. The multi-objective optimization model is expressed as [9]

$$\begin{cases} \text{find} & \boldsymbol{\alpha} \in \boldsymbol{E}^n \\ \min & \left\| \Delta y^c - \Delta y^p \right\|_2 \\ \min & \left\| \boldsymbol{\alpha} \right\|_0 \\ \text{s.t.} & \alpha_l \le \alpha_i \le \alpha_u \end{cases} \tag{13}$$

where $\|\cdot\|_p$ denotes the l_p norm. Here we select l_0 norm of $\boldsymbol{\alpha}$ aiming at dealing with the sparsity of the damage index vector.

As a representative approach developed, here we adopt the particle swarm optimization (PSO) [10] as to solve the optimization problem presented above. In the case of damage identification, there are many elements/segments to be identified, i.e., many unknowns. Besides, the resulting multi-modal objective function has many local extremes so that the PSO algorithm may get stuck in the local minima, thus leading to incorrect identified solutions. To address the challenges, a series of local search strategies are proposed to enhance the global searching ability of PSO algorithm in this section. Furthermore, Q-table is employed to select the proper strategy for the particle at each iteration to prevent the particle from entrapment of local extreme.

Framework of proposed memetic optimizer Particle swarm optimization (PSO) algorithm is a stochastic optimization technique based on swarm, which was originally proposed by Eberhard and Kennedy. PSO is based on extrinsic behavior of population. In standard PSO the particles are manipulated by the following Equations (14) and (15). In PSO algorithms, each solution is like a 'bird', and each bird 'flies' around in the multidimensional problem space with an acceleration.

$$v_i(t+1) = sv_i(t) + c_1 r_1\left(p_{\text{best}i}(t) - x_i(t)\right) + c_2 r_2\left(g_{best}(t) - x_i(t)\right) \tag{14}$$

$$x_i(t+1) = x_i(t) + v_i(t+1) \tag{15}$$

The coefficient *s* is the inertia weight, c_1 is coefficient for cognitive component which indicates that each particle learns from its experiences, and c_2 is coefficient for social component from which each particle will learn. *v* is velocity of particle, *x* is position of particle or solution for the optimization problem, r_1 and r_2 are random numbers, *t* is the current iteration, p_{best} is the personal best, and g_{best} is the global best.

PSO or Multi-objective Particle Swarm Optimization (MOPSO) algorithm often falls into entrapment of swarm within local minima of search space [11]. Moreover, it may achieve a premature convergence though it has several advantages such as its effectiveness, robustness, simplistic implementation. Besides, proper control should be exerted for exploration and exploitation. The algorithm may get trapped in the local minima for the functions with multi-modal characteristics. This problem will become more severe with the dimensional increase of the optimization problem. For example, in damage identification using piezoelectric admittance, large number of finite elements and large number of segments are employed to ensure satisfying accuracy of the finite element model and the capability of identifying small-sized damage more elements in finite element analysis. To tackle these challenges, a series of local search strategies are developed. The strategies in this research are Exploration, Convergence, High/Low Jump. Exploration and Convergence are two similar updating strategies with different cognitive and social coefficients used to achieve a dynamic updating process, in which the search starts with exploration and converges at the end of search process. High/Low Jumpy conducts a mutation for one of the dimensions of personal best to make the particle take a large/small walk to see if it can jump out of current personal best.

The suggested range for inertia weight is $s \in [0.4, 0.9]$ [10]. It is noteworthy that *s* must be high in the exploration and low in convergence. For coefficients c_1 and c_2, they control the balance

between p_{best} and g_{best}. Therefore, c_1 must be higher than c_2 in exploration and the opposite in the convergence [12, 13]. For the 'Exploration', we now set coefficients in Equation (14) as $s = 0.8$, $c_1 = 2.5$, $c_2 = 0.5$, as used in literature [14,15]. In the 'Convergence' state, the algorithm will converge to the global best quickly, therefore, the social part now is given a larger value, so the coefficients are 0.4, 0.5, 2.5 respectively for w, c_1 and c_2. For the High/Low Jump, one of the dimensions of the personal best is randomly selected and perturbed using Gaussian distribution. The only difference between High and Low Jump is the standard deviation is larger for High Jump. Here we use 0.9 for High Jump and 0.1 for Low Jump. The mathematic expression can be denoted as [16]

$$x_i = P_{besti} + R_{norm}\left(V_{upper} - V_{lower}\right) \tag{16}$$

where R_{norm} is a random number sampled from Gaussian distribution $N \square \left(\mu, \sigma^2\right)$. The mean values for both High and Low Jump are zero.

Since the particle cannot execute all local search strategies at one time (iteration), Q-table here is combined to help particle select the proper local strategy based on the maximum Q-table value, as shown in Figure 1. To elaborate on the memetic optimizer, we summarize the algorithm as the following

Step 1: Initialize all the necessary parameters, such as # of objectives, # of population, # of variables (dimension), searching bounds, maximum iterations, etc.

Step 2: Initialize population using random number within searching space. Initialize Q-table all zeros with dimension 4 by 4. Initialize personal best, global best. Initialize local strategy as 'Exploration'.

Step 3: Main loop for MOPSO algorithm until maximum iteration is reached: Executing 'Exploration' and using Non-dominated Sorting algorithm to determine if the updated solution is kept or ignored. If the newly generated solution is kept, an immediate reward is given, or a penalty will be given. The reward or penalty will be used to update the Q-table value (will be discussed in following subsection). Executing other local strategies based on maximum Q-table values until maximum iteration is reached.

Step 4: Updating personal best if newly obtained solution is kept or do nothing. Updating global best and Pareto solution repository.

Step 5: Solution visualization and interpretation.

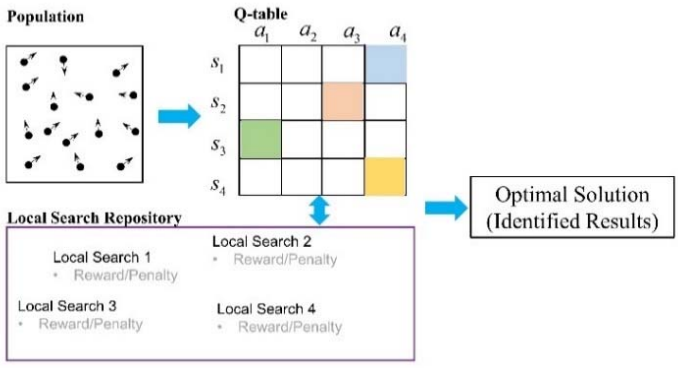

Figure 9 Q-table interaction with local strategies

Local search strategy selection Local searching strategies are proposed here to help particles jump out of local minima to achieve a global search. However, all the strategies cannot be executed at the same time. Thus, Q-table here is selected to achieve the dynamic selection goal. Q-table is usually used in Q-learning, in which the learner performs an action causing a state transition in the environment it resides and receives a reward or penalty for the action executed to reach a definite goal [15,17,18]. Here the particle is regarded as agent and the local strategies are actions.

The current state is set as Exploration because the particle is hoped to explore more searching space at the beginning of the algorithm. In the main iteration part, the particle will select the action which has the maximum value in the Q-table and execute the action. After executing the current action, the agent can get to the new state using observing function $o(s,a)$ which makes a transition from current state to another. The transition here is that current action index is the next state index. Here a diagram is drawn to show how to switch from current state to next state. As shown in Figure 10, the agent will select an action based on the maximum table values given the current s_1. For example, if Action 3 (a_3) has a maximum value and then the next state will be set as s_3, which has the same index to the index of current action a_3. This process can be written mathematically as

$$a_t = index\left\{\max\left(Q\left(s_t, actions\right)\right)\right\} \tag{17}$$

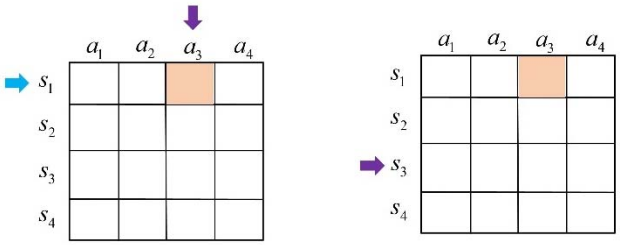

Figure 10 State transition process.

After Action 3 is executed, the rewards obtained currently can be passed into Equation (18) to update the entry for the current state and current action. Then the personal best and the global best are updated, and the external optimal repository will be updated accordingly. All the steps in the main loop will be performed until maximum runs are reached. There are 4 states and their corresponding actions. Therefore, we can create a Q-table with size 4 by 4 and initialize all the entries as zeros. Usually, the current state is randomly chosen from the state repository. However, here we initialize the current state as 'Exploration' since we hope the algorithm starts with exploring more searching space. Then the best action will be selected and executed based on the maximum Q-table value given the current state.

After executing the selected action, an immediate reward or penalty will be obtained. Reward or penalty is determined by the solution dominating algorithm. If the new solution dominates the old solution, then a positive value 1 is given as a reward, otherwise, a negative reward -1 is given as penalty. And then observe the maximum future reward under the next state (next state index is same to the current action index, referring to Figure 10) and this reward will be passed into the updating function to update the Q-table entry $Q(s_t, a_t)$. The updating function is

$$Q_{new}(s_t, a_t) = (1-\alpha) Q(s_t, a_t) + \alpha \left[r_{t+1} + \gamma \max_a Q(s_{t+1}, a_{all}) \right] \quad (18)$$

where α is called the learning rate, which is defined as how much the new value vs the old value is accepted. γ is a discount factor. It is used to balance immediate and future reward. *r* is the value after completing a certain action at a given state. Max is operation to take the maximum of the future reward and apply it to the reward for the current state. Finally, the current state will be updated as current state

A number of case analyses are conducted to examine the proposed algorithm improvements in multi-objective optimization for damage identification. A cantilevered aluminum structure is integrated with a single piezoelectric transducer, as shown in Figure 3. The dimension of the beam is specified as length 561 mm, width 19.05 mm and thickness 4.763 mm. The density and Young's modulus are 2700 kgm^{-3} and 68.9 GPa, respectively. The piezoelectric transducer is placed at 180 mm from the left end, with length 15 mm, width 19.05 mm, and thickness 4.763 mm. The Young's moduli of piezoelectric transducer are Y_{11} = 86 GPa and Y_{33} = 73 GPa, and the density is 9500 kgm^{-3}. The piezoelectric constant and dielectric constant are $h_{31} = -1.0288 \times 10^9 \, Vm^{-1}$ and $\beta_{33} = 1.3832 \times 10^8 \, mF^{-1}$, respectively.

Without loss of generality, admittance changes are acquired around the 14th (1893.58 Hz) and the 21st (3704.05) natural frequencies. Two frequency ranges are selected from 1891.69Hz to 1895.47Hz and from 3700.35Hz to 3707.75Hz with 100 sweeping points for each range. Two damage cases are considered. The first case is dividing the plate into 225 segments, each corresponding to a damage index to be identified, as shown in Figure 11(a) and the damage is assumed at segment 75 with 13.2% stiffness reduction. For the second case, the segment is much finer, resulting in 1125 segments (Figure 11(b)) and the damage is located at segment 800 with 9.5% stiffness reduction.

Table 1 Damage identification results

Case #	Solutions	Obj-fun 1	Obj-fun 2
Case 1	1	8.864434e-6	1
	2	8.864416e-6	2
Case 2	1	5.623299e-6	2
	2	2.197487e-7	2

The total number of admittance measurement data points are 200 for both cases. We can see that the damage identification for both cases are under-determined or the information for damage identification is limited. It should be mentioned that damage usually occurs at a small region of the structure, thus resulting in a sparse damage index vector. We use the sparse initialization algorithm that can generate the sparse population. Then it will be passed into the main optimization loop. By solving the optimization model formulated in Section 2 using the proposed algorithms, the identified results are obtained for both cases, as plotted in Figures 5 and 6. The figures are arranged based on the non-zero identified segments (the second objective function.). The obtained solutions for both cases are summarized in Table 1.

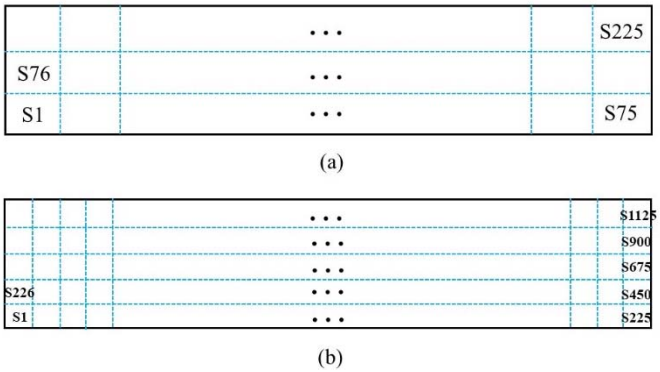

Figure 11 Segment division a) coarse division (Case 1); and b) fine division (Case 2).

For Case 1, the two optimal solutions obtained accurately pinpoint the true damage location and severity. The two solutions manifest the characteristic of underdetermined problem that has multiple solutions. Though there is a misidentified damage location in solution 2 at segment 26, as plotted in Figure 12, the misidentified damage has a negligible severity that reflects the modeling errors in finite element analysis. Besides, we use the Tylor series expansion to obtain the linear relationship between damage index and admittance change. Since we do not know the information about the damage, both solutions obtained, therefore, can be regarded as possible candidates for engineering practice.

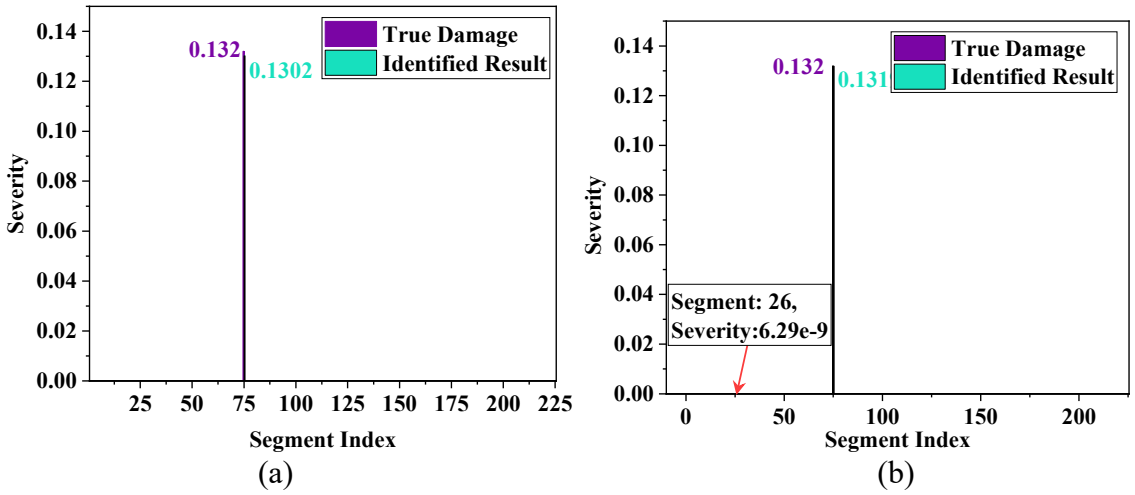

Figure 12 Damage identification results for Case 1 with 225 segments.

As mentioned, modeling error and linear approximation may lead to misidentified damage locations, which is also reflected in the two solutions of Case 2, as shown in Figure 13. Each solution has two identified damage locations. One precisely captures the true damage scenario, and the other is the misclassified damage location. Within the multi-objective optimization setup, multiple solutions can be obtained for underdetermined problem and there is always one solution that captures the true damage scenario. In this case, both solutions can be regarded as possible candidate in practical problems.

In this research, case studies demonstrate the global searching ability of proposed memetic optimizer, which performs well in damage identification problems with underdetermined characteristics.

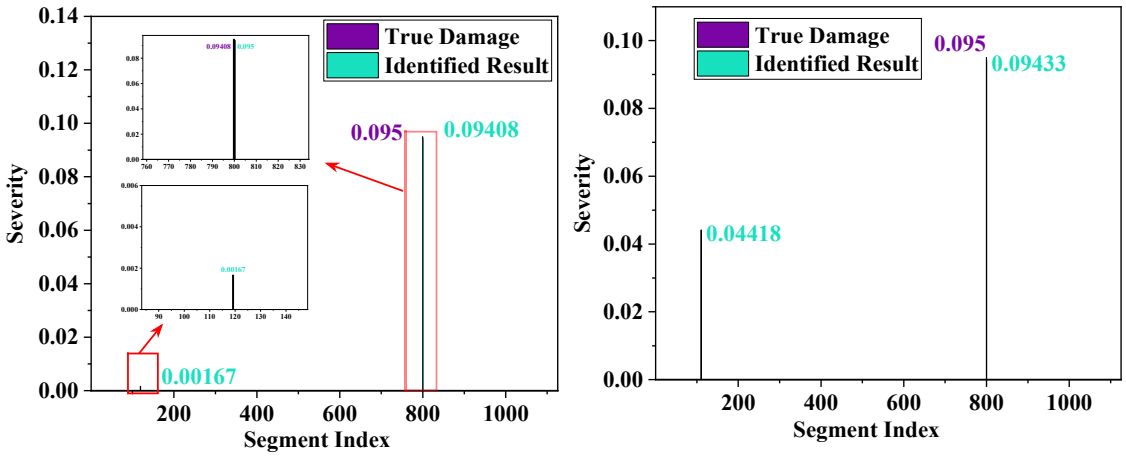

Figure 13 Damage identification results for Case 2 with 1125 segments.

A memetic optimizer based on MOPSO algorithm is presented for damage identification using electromechanical admittance measurements. The inverse damage identification process is converted into an optimization problem. Given that the algorithm solving optimization model usually falls into the local extremes and get a premature convergence, a series of local search strategies are proposed aiming at enhancing the global searching ability when dealing with multi-modal objective function. The Q-table is utilized here to help the particle to select the proper local search based on maximum Q-table values. Case demonstrations verify the validity of the algorithm.

In summary, in this research, we systematically design and analyze piezoelectric impedance/admittance based active interrogation, synthesize self-powering scheme to increase electromechanical coupling of the transducer, formulate effective and robust damage identification algorithms utilizing sensor measurement as input. Our results indicate that piezoelectric active interrogation is a viable option for damage identification of large-scale infrastructure component, and the associated damage identification inverse analysis based on multi-objective optimization can pinpoint damage location and quantify severity.

Chapter 4: Education Impact and Knowledge Dissemination

Throughout this project, three graduate students are involved at different stages of research. Yixin Yao developed sensor modeling as well as ultrasound wave analysis. He gathered industry insight on ultrasound based railway track inspection, and incorporated the understanding into the project development. He received the M.S. degree in Mechanical Engineering in December 2020. Ting Wang, a Ph.D. student in Mechanical Engineering, developed piezoelectric energy harvesting for enhancing electromechanical coupling by utilizing negative capacitance. Yang Zhang, a Ph.D. student in Mechanical Engineering, formulated a series of damage identification algorithms. Ting Wang and Yang Zhang jointly developed the experimental testbed for piezoelectric admittance based sensory system. The results will be included in their respective Ph.D. dissertations.

The research findings have been integrated into several undergraduate- and graduate-level classes that the PI has instructed in research years, including ME3220 Mechanical Vibrations, ME 5420 Advanced Mechanical Vibrations, ME 5210 Intelligent Material Systems and Structures, ME 5895 Structural Dynamics, and ENGR3195/5300 Industry 4.0.

The research outcome has been summarized into a number of conference and journal publications:

- Zhang, Y., and Tang, J., "Structural damage identification using multi-objective optimization based inverse analysis," Proceedings of SPIE, Smart Structures / NDE, V11380, 2020. (The result was presented in the conference)

- Wang, T., Dupont, J., and Tang, J., "Enhanced passive vibration suppression using self-powered piezoelectric circuity integration," Proceedings of SPIE, Smart Structures / NDE, V12043, 2022. (The result was presented in the conference)

- Zhang, Y., Zhou, K., and Tang, J., "Structural damage identification using inverse analysis through optimization with sparsity," Proceedings of SPIE, Smart Structures / NDE, V12046, 2022. (The result was presented in the conference)

- Wang, T., and Tang, J., "Parametric analysis of negative capacitance circuit for enhanced vibration suppression through piezoelectric shunt," Proceedings of the ASME 2022 International Design Engineering Technical Conferences and Computers and Information in Engineering Conference IDETC/CIE2022, DETC2022-90616. (The result was presented in the conference)

- Wang, T., Dupont, J., and Tang, J., "On integration of vibration suppression and energy harvesting through piezoelectric shunting with negative capacitance," IEEE/ASME Transactions on Mechatronics, submitted.

- Zhang, Y., Zhou, K., Ball, A., and Tang, J., "Reinforcement learning guided multi-objective particle swarm optimization for fault identification using electromechanical impedance measurements, in preparation to be submitted to Mechanical Systems and Signal Processing.

The research results have also been shared with the community in TIDC annual review meetings.

Chapter 5: Conclusions and Recommendations

The objective of this project is to synthesize novel sensors integrated with physics-informed data analytics to facilitate damage identification of infrastructure components. The efforts encompass new active sensing mechanisms development and new physics-informed inference algorithms formulation.

Our findings are the following:

- Piezoelectric impedance/admittance measurements can be effectively acquired based on simple circuitry design.
- The impedance/admittance measurements can be acquired in high frequency range which carry the damage signature with high precision.
- The piezoelectric transducer employed in the active interrogation scheme can be concurrently utilized for energy harvesting.
- Upon proper circuitry synthesis, the electromechanical coupling of the piezoelectric transducer can be increased with the incorporation of negative capacitance element.
- The negative capacitance integration can be designed self-sustainable with positive net power upon energy harvesting.
- Using piezoelectric impedance/admittance measurements as input, multi-objective optimization algorithms are capable to identifying the location and severity of structural damage with high accuracy and robustness.

With these results, we conclude that the proposed piezoelectric active interrogation can be a viable option for the damage identification of large scale infrastructure components.

The design and analysis methodology formulated in this research lays down a foundation for engineering implementation. In order to fully unleash the potential of the new technology, we envision the following further advancements:

- The sensor nodes can be made wireless by the integration of wireless communication module.
- Currently the sensing system is capable of identifying damage location and severity in terms of local stiffness reduction. Future investigation may focus on further identifying the type and physical mechanism of damage. This can be realized by means of heterogeneous sensing with multiple types of sensing mechanisms.
- Future investigation may also focus on detecting and identifying progressive damage to realize damage prognosis.

References

[1] Shuai, Q., Zhou, K., Zhou, S. and Tang, J., Fault identification using piezoelectric impedance measurement and model-based intelligent inference with pre-screening. Smart Materials and Structures, 26(4), p.045007, 2017.

[2] Zhang, Y., and Tang, J., "Structural damage identification using multi-objective optimization based inverse analysis," Proceedings of SPIE, Smart Structures / NDE, V11380, 2020.

[3] Zhang, Y., Zhou, K., and Tang, J., "Structural damage identification using inverse analysis through optimization with sparsity," Proceedings of SPIE, Smart Structures / NDE, V12046, 2022.

[4] S.A. Mansoura, P. Bénard, B. Morvan, P. Maréchal, A.C. Hladky-Hennion and B. Dubus, "Theoretical and experimental analysis of a piezoelectric plate connected to a negative capacitance at MHz frequencies," Smart Mater. Struct., vol.24, pp. 115032-115038, 2015.

[5] B. Götz, M. Schaeffner, R. Platz, and T. Melz, "Lateral vibration attenuation of a beam with circular cross-section by a support with integrated piezoelectric transducers shunted to negative capacitances," Smart Mater. Struct., vol. 25, no. 9, pp.095045-095054, 2016.

[6] Wang, T., Dupont, J., and Tang, J., "Enhanced passive vibration suppression using self-powered piezoelectric circuity integration," Proceedings of SPIE, Smart Structures / NDE, V12043, 2022.

[7] J. Tang, K.W. Wang, "Active-passive hybrid piezoelectric networks for vibration control: comparisons and improvement," Smart Mater. Struct., vol. 10, no. 4, pp. 794-806, Aug. 2001.

[8] Wang, T., and Tang, J., "Parametric analysis of negative capacitance circuit for enhanced vibration suppression through piezoelectric shunt," Proceedings of the ASME 2022 International Design Engineering Technical Conferences and Computers and Information in Engineering Conference IDETC/CIE2022, DETC2022-90616.

[9] Zhang, Y., Zhou, K., and Tang, J., "Structural damage identification using inverse analysis through optimization with sparsity," Proceedings of SPIE, Smart Structures / NDE, V12046, 2022.

[10] Kennedy, J. and Eberhart, R., November. Particle swarm optimization. In Proceedings of ICNN'95-international conference on neural networks, 4 1942-1948), 1995.

[11] Coello, C.A.C., Pulido, G.T. and Lechuga, M.S., Handling multiple objectives with particle swarm optimization, IEEE Trans Evol Comput, 8.3 (2004): .256-279.

[12] Zhan, Z.H., Zhang, J., Li, Y. and Chung, H.S.H, Adaptive particle swarm optimization, IEEE Trans. Syst. Man Cybern, 39. 6 (2009): 1362-1381.

[13] Wang, Y., Li, B., Weise, T., Wang, J., Yuan, B. and Tian, Q, Self-adaptive learning based particle swarm optimization, Inf. Sci, 181.20 (2011): 4515-4538.

[14] Ratnaweera, Asanga, Saman K. Halgamuge, and Harry C. Watson, Self-organizing hierarchical particle swarm optimizer with time-varying acceleration coefficients, IEEE Trans. Evol. Comput, 8.3 (2004): 240-255.

[15] Samma, Hussein, Chee Peng Lim, and Junita Mohamad Saleh, A new reinforcement learning-based memetic particle swarm optimizer, Appl. Soft Comput, 43 (2016): 276-297.

[16] Lim, Wei Hong, and Nor Ashidi Mat Isa, Two-layer particle swarm optimization with intelligent division of labor, Eng. Appl. Artif. Intell., 26.10 (2013): 2327-2348.

[17] Meerza, Syed Irfan Ali, Moinul Islam, and Md Mohiuddin Uzzal, Q-learning based particle swarm optimization algorithm for optimal path planning of swarm of mobile robots, 2019 1st International Conference on Advances in Science, Engineering and Robotics Technology (ICASERT). IEEE.

[18] Watkins, Christopher JCH, and Peter Dayan, Q-learning, Mach. Learn., 8.3 (1992): 279-292.

Transportation Infrastructure Durability Center
AT THE UNIVERSITY OF MAINE

35 Flagstaff Road
Orono, Maine 04469
tidc@maine.edu
207.581.4376

www.tidc-utc.org